Hard and Flexible Nanocomposite Coatings using Nanoclay-Filled Hyperbranched Polymers

Linda Fogelström, Eva Malmström, Mats Johansson, and Anders Hult*

KTH Fibre and Polymer Technology, School of Chemical Science and Engineering, Royal Institute of Technology, SE-10044 Stockholm, Sweden

ABSTRACT The combination of hardness, scratch resistance, and flexibility is a highly desired feature in many coating applications. The aim of this study is to achieve this through the introduction of an unmodified nanoclay, montmorillonite (Na^+MMT), in a polymer resin based on the hyperbranched polyester Boltorn H30. Smooth and transparent films were prepared from both the neat and the nanoparticle-filled hyperbranched resins. X-ray diffraction (XRD) and transmission electron microscopy (TEM) corroborated a mainly exfoliated structure in the nanocomposite films, which was also supported by results from dynamic mechanical analysis (DMA). Furthermore, DMA measurements showed a 9−16 °C increase in Tg and a higher storage modulus−above and below the T_g−both indications of a more cross-linked network, for the clay-containing film. Thermogravimetric analysis (TGA) demonstrated the influence of the nanofiller on the thermal properties of the nanocomposites, where a shift upward of the decomposition temperature in oxygen atmosphere is attributed to the improved barrier properties of the nanoparticle-filled materials. Conventional coating characterization methods demonstrated an increase in the surface hardness, scratch resistance and flexibility, with the introduction of clay, and all coatings exhibited excellent chemical resistance and adhesion.

KEYWORDS: nanocomposites • hyperbranched polymers • montmorillonite • coatings • mechanical properties • thermal properties • barrier properties

1. INTRODUCTION

The combination of hardness, scratch resistance, and flexibility is a highly desired feature in many different coating applications. A potential route to achieve this aim is via the introduction of a nanoparticle filler into the polymer resin. Expandable layered silicate clays, with montmorillonite (MMT) as a typical example (1), are among the most commonly used nanofillers for polymer nanocomposites. Polymer/layered silicate nanocomposites can either be referred to as intercalated if the polymer is present between the clay layers, but the regularity of the layered structure is maintained, or as exfoliated if the clay layers are completely dispersed in the matrix (2). To fully utilize the property-improving potential of the nanofiller, complete dispersion is necessary, so that the entire surface area of the nanosized clay particles is available to interact with the polymer. The great interest for using nanoparticles to reinforce polymers emerged in the late 1980s when a research group from Toyota reported their findings regarding the possibility of building a nanostructure from a polymer and an organophilic clay, with dramatic property improvements (3, 4). Since then, improvements in mechanical properties (5−12), barrier properties (6, 13−17), thermal properties (18−24), and optical properties (25−27) have been reported for a variety of different polymers−generally at very low filler loadings. Various methods have been employed to prepare polymer/clay nanocomposites. The first method, used by the Toyota group, was the in situ synthesis (25, 28−30). In this method the polymerization is initiated in between the clay layers, and the polymer build-up causes the interlayer gallery to expand. Another commonly used method is the melt processing technique, in which the clay is dispersed in a polymer in the molten state, using high shear forces and high temperatures (9, 31−33). The above-described nanocomposite preparation methods generally require modification of the naturally hydrophilic clay to improve the compatibility with the polymer. However, this modification could be avoided using the solution intercalation method with water as solvent, thereby making use of native MMT's affinity for water and its ability to exfoliate in aqueous solutions (34, 35). Linear water-soluble polymers, processed with this method, have in some cases resulted in reaggregated intercalated structures, rather than exfoliated structures, after drying (36, 37). The use of dendritic polymers such as hyperbranched polyesters, on the other hand, has been shown to promote exfoliation and stabilize the exfoliated structure after drying (38−40). This stabilization is thought to be enabled by the compact globular structure of the hyperbranched polymer, with a large number of polar end-groups and a relatively hydrophobic core, preventing the molecule from collapsing onto the clay layers (41). Furthermore, the unique features of dendritic polymers are also very favorable in coating applications; in addition to the large number of end-groups, offering versatile cross-linking possibilities, the globular structure of dendritic polymers enables a maintained low viscosity even at high molecular weights (42). A

* Corresponding author. E-mail: andult@kth.se.
Received for review March 9, 2010 and accepted May 5, 2010
DOI: 10.1021/am1001986

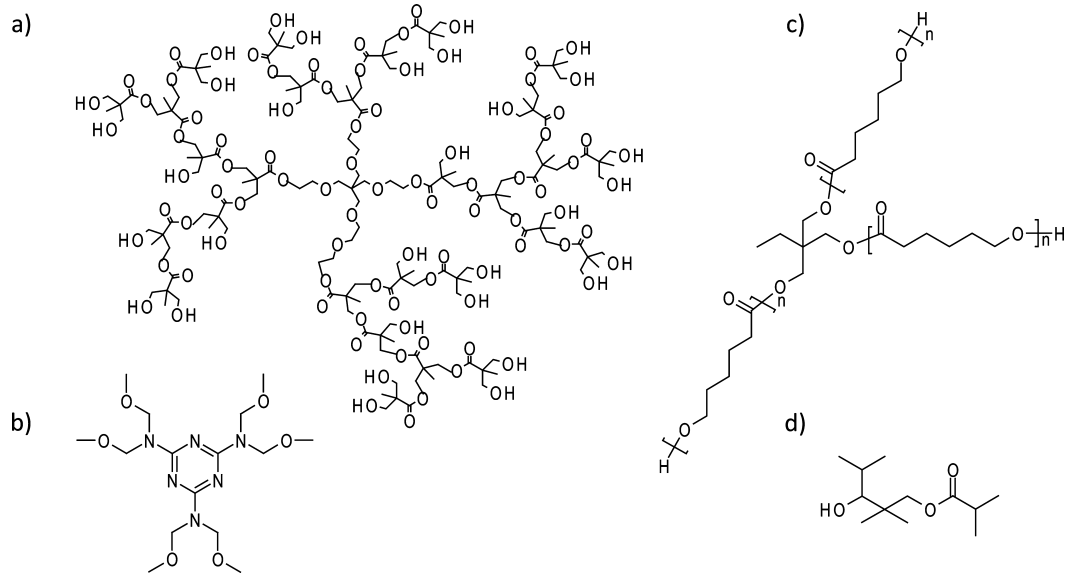

FIGURE 1. (a) Boltorn H30, (b) HMMM, (c) TONE polyol 0301, $n \approx 2$, (d) Texanol.

recent study (43), published in Nature, demonstrates the versatility of using native MMT in combination with a dendritic polyester based on 2,2- bis(methylol)propionic acid (Bis-MPA) yielding a high-water-content, moldable, self-healing hydrogel with excellent mechanical strength.

The aim of this study is to design a hard and scratch resistant coating, with maintained flexibility, through the introduction of a nanoparticle filler in a polymer resin based on the hyperbranched polyester Boltorn H30 (44), thermally cured with hexakis(methoxymethyl)melamine (HMMM) as cross-linker.

2. EXPERIMENTAL SECTION

2.1. Materials. The hyperbranched polymer Boltorn H30, a dendritic polyester based on the AB2-type monomer 2,2-bis(methylol)propionic acid (Bis-MPA), was kindly supplied by Perstorp AB Sweden. The clay used is a natural montmorillonite (Na^+MMT) from the Cloisite nanoclays series by Southern Clay Products, with a *d*-spacing of 11.7 Å according to SCP's X-ray results. hexakis(methoxymethyl)melamine (HMMM) was supplied by Becker Industrial Coatings AB, and epoxy-blocked p-toluenesulfonic acid (epoxy-blocked pTSA) was supplied by Akzo Nobel Nippon Paint AB. TONE polyol 0301 was purchased from Union Carbide, and 2,2,4-trimethyl-1,3-pentanediol monoisobutyrate (Texanol) was purchased from Sigma-Aldrich.

2.2. Instruments and Analyses. X-ray diffraction (XRD) analysis was performed on the cured coatings with a PANalytical XPert Pro powder diffractometer in reflection mode, using copper-radiation, $CuK_{\alpha 1}$ ($\lambda \approx 1.5406$ Å). Transmission electron microscopy (TEM) analysis was performed on a Philips Tecnai 10, using an acceleration voltage of 80 kV. The TEM samples were prepared from the cured coatings, cast in epoxy and cut with an ultramicrotome. The tensile properties of the coatings were measured on freestanding films with dynamic mechanical analysis (DMA), TA Instruments Q800. Thermogravimetric analysis (TGA) was performed on a Mettler Toledo TGA/SDTA851^e instrument. The samples were heated from 40 to 800 °C with a heating rate of 10 °C/min, and a N_2 or O_2 flow of 50 mL/min. Conventional coating characterization methods: pendulum hardness was studied with a 299 Koenig pendulum hardness tester from Erichsen; pencil hardness tests were principally performed according to SIS 18 41 87 standard, using pencils manufactured by KOH-I-NOOR; scratch tests were principally performed according to ISO 2409 standard, using a multiedge cutting tool and a brush, both manufactured by Erichsen; chemical resistance was analyzed through the MEK-rub test, using methyl ethyl ketone as solvent.

2.3. Preparation of Boltorn H30 and Na^+MMT Nanocomposites. The method for preparing nanocomposites from Boltorn H30 and Na^+MMT was adopted from Månson et al. (38) Boltorn H30 (19.7 g/19.1 g) was added to a round-bottomed flask, and preheated in an oven at 140 °C until it melted, in order to break the hydrogen bonds present in the material (45−47). Deionized water (150 mL) was added and the flask, with a stopper, was put in an oil bath at 100 °C and the mixture was kept under stirring. When a cloudy solution was obtained, Na^+MMT (0.31 g/0.92 g) predispersed in boiling deionized water (50 mL) was added and dispersed in the polymer solution under vigorous stirring. After 1 h, the temperature was reset to 50 °C, the stopper removed, and the mixture was kept stirring until most of the water had evaporated. The resulting "gel" was transferred to a silicon rubber mold and dried in air at 50 °C for 2 days and under a vacuum at 50 °C for another 2 days.

2.4. Nanocomposite Preparation of Boltorn H30 and Na^+MMT for Thermal Analysis. Nanocomposites of Boltorn H30 with Na^+MMT contents of 1, 2, 5, and 10 wt %, respectively, were prepared according to the method described in section 2.3.

2.5. Coating Preparation. Coatings with and without nanofiller were prepared in the same way. Boltorn H30 or nanocomposite, as prepared in section 2.3, (1.95 g) was preheated and dissolved in methanol (3.8 mL). HMMM (0.45 g) and TONE polyol 0301 (0.60 g) were added, together with Texanol (ca. 30 μL) and a catalytic amount of the epoxy-blocked pTSA. Films were applied to glass substrates (for the pendulum hardness and MEK-rub tests), steel substrates (for the pencil hardness and scratch tests) and nonstick-coated steel substrates (to obtain freestanding films for XRD, TEM and DMA) and cured in an oven at 140 °C for 20 min. The resulting thickness for all coatings were ca. 50 μm and the final Na^+MMT contents in the nanoparticle-filled coatings were 1 and 3 wt %, respectively.

3. RESULTS AND DISCUSSION

Nanocomposites based on Boltorn H30 and Na^+MMT were prepared and used for coating applications.

Coatings were prepared from neat Boltorn H30 (Figure 1a), and the nanocomposites of Boltorn H30 and Na^+MMT,

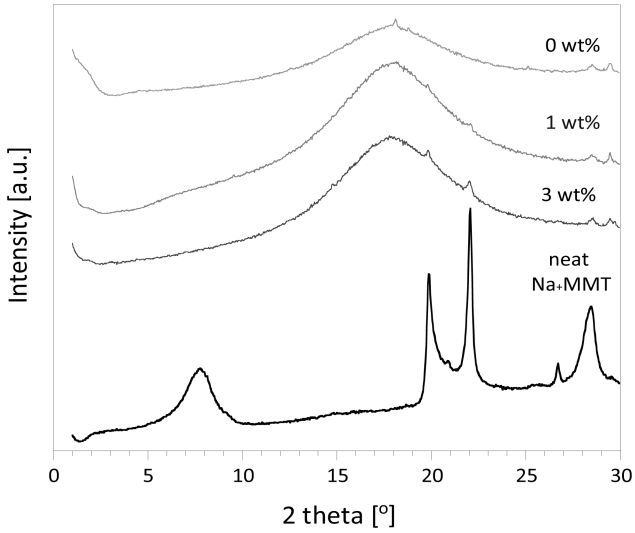

FIGURE 2. XRD spectra of neat Na^+MMT and Boltorn H30 coatings with 0, 1, and 3 wt % Na^+MMT.

using HMMM (Figure 1b) as cross-linker in all formulations. The polyol TONE 0301 (Figure 1c) was added to increase the flexibility of the coating in order to facilitate the investigation of the influence of the nanofiller; since the nanofiller mainly affects the rubber plateau, the influence will be larger on soft and flexible materials. To avoid premature cross-linking, we used a blocked version of the catalyst pTSA, which is not activated until subjected to higher temperatures, i.e., in the curing oven. Texanol was added to facilitate the film-forming process, in order to obtain uniform and smooth films (48). Three different coatings were prepared, with 0, 1, and 3 wt % clay, respectively.

The cross-linking of hydroxyl-functional polyesters with HMMM is a conventional approach to thermally cured coating systems. The cross-linking proceeds through an etherification reaction, in which the nucleophilic hydroxyl-groups on Boltorn H30 attack the methoxy-groups on HMMM and methanol is released (49). This reaction is relatively insensitive to residual water, because a primary hydroxyl-group is a much stronger nucleophile than a water molecule.

3.1. Nanocomposite Characterization. Freestanding films were obtained by peeling off the cured coatings from the nonstick coated steel substrates. The dispersion of the clay layers in the nanofilled coatings was investigated with XRD and TEM. The large peak at 8° in the XRD spectrum of neat clay, Na^+MMT, in Figure 2 represents the regular distance between the clay layers. This peak cannot be seen in any of the spectra of the prepared nanocomposites, strongly indicating that the regularity of the layered clay structure is broken, and that a mainly exfoliated structure is obtained in both materials. The peaks at 20 and 22° in the Na^+MMT spectrum can be used to verify that the clay content in the prepared nanocomposite materials is higher than the detection limit; these peaks represent smaller distances within the clay layers and would therefore remain even if the clay layers are dispersed, and an exfoliated structure is obtained. As can be seen, the peaks at 20 and 22° are visible in the spectra of both prepared nanocomposites, confirming that the clay content is above the detection limit in these materials.

Figure 3, showing representative micrographs of the structures of the clay-containing materials, corroborate the XRD results; both of the nanofilled coatings exhibit a mainly exfoliated structure.

Nanocomposites of clay-filled Boltorn H30, as well as references of neat hyperbranched polymer and neat clay, were analyzed with TGA, both under nitrogen and oxygen flow, Figure 4a,b. When subjecting the material to a flow of nitrogen during the analysis, the mechanism for the thermal degradation is pure pyrolysis, and when an oxygen flow is used, the thermal degradation proceeds through oxidative combustion. In the thermograms where nitrogen has been used, i.e., where the material has undergone pure pyrolysis, there are no significant differences in between the samples. In oxygen atmosphere, on the other hand, a significant difference is observed between the thermogram of the pure hyperbranched polymer and the thermograms of the nanocomposites; taking the temperature when 50% of the material is degraded as a reference point, a temperature shift

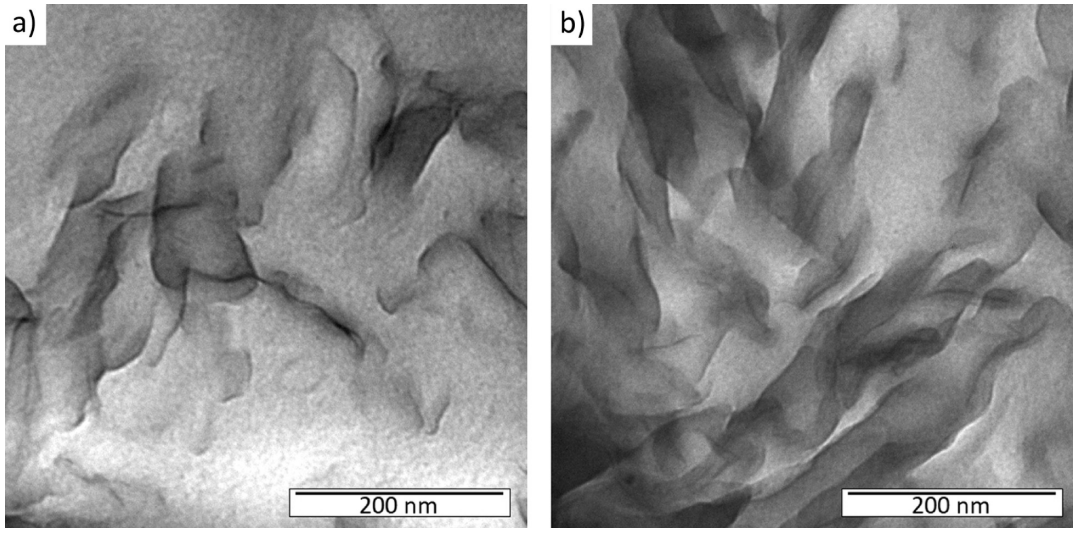

FIGURE 3. TEM micrographs showing Boltorn H30 coatings with (a) 1 and (b) 3 wt % Na^+MMT.

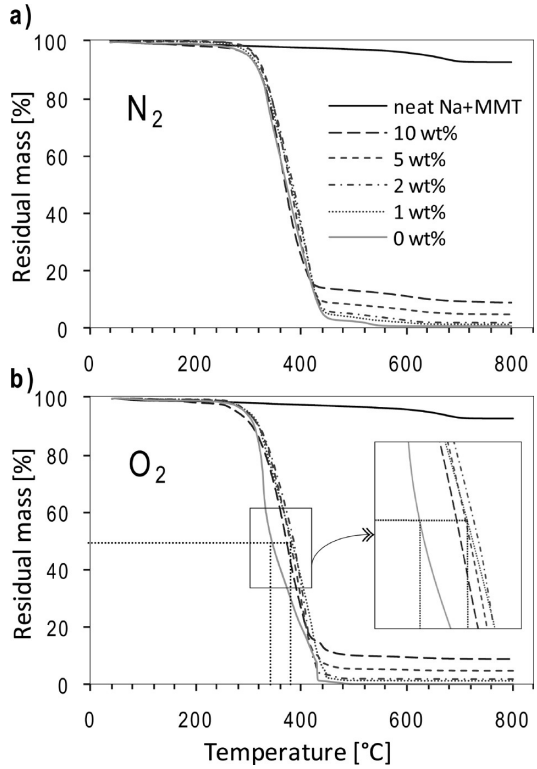

FIGURE 4. TGA results of neat Boltorn H30, Boltorn H30 with different Na^+MMT loadings and neat Na^+MMT in (a) nitrogen atmosphere and (b) oxygen atmosphere. The legend in a is valid for both thermograms.

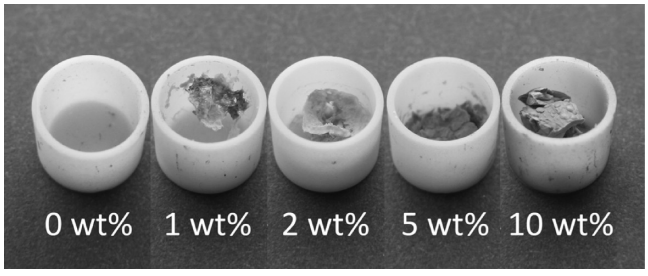

FIGURE 5. Photograph showing TGA samples of Boltorn H30, with different Na^+MMT loadings, after analysis in oxygen atmosphere.

of approximately 40 °C can be seen between the neat hyperbranched polymer (ca. 340 °C) and the nanocomposites (ca. 380 °C). The degradation onset temperature, however, is similar for all of the prepared materials. This means that although the thermal degradation of the materials starts at the same temperature, the oxidative degradation process is delayed in the nanocomposite materials, an effect that could be attributed to the improved barrier properties of the nanocomposites; the sheetlike clay nanoparticles effectively hinder the diffusion of oxygen molecules in the material. However, at the same time as the clay nanosheets decrease the permeability of molecules penetrating into the material, they also restrict the out-diffusion, for example, of water molecules, which affects the drying of the material. The residual moisture in turn greatly affects the barrier properties of the matrix material; in the dry state the hydroxyl-functional hyperbranched polymer is an excellent oxygen barrier in itself, but moisture has a documented negative impact on the barrier properties of this type of material (50).

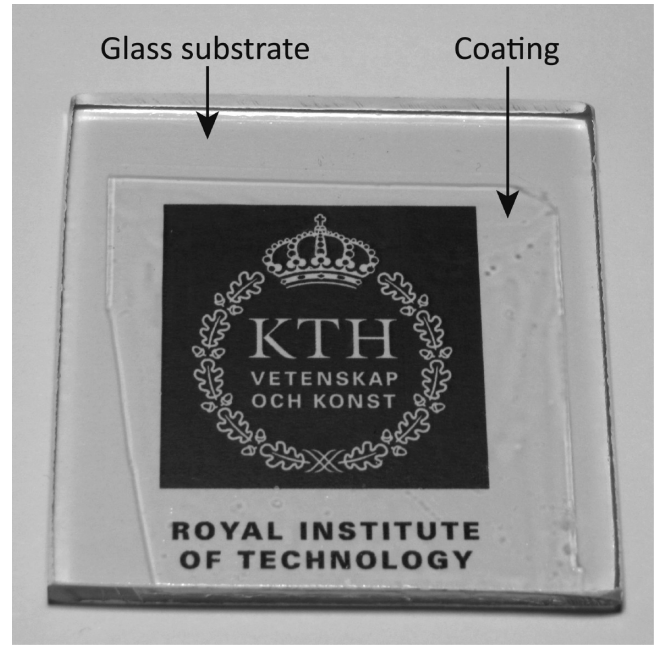

FIGURE 6. Smooth and transparent coating of Boltorn H30 with 2 wt % Na^+MMT.

This means that nanoclay has a conflicting influence on the permeability in this type of material, which in the TGA results is expressed as an apparent maximum in the nanoclay's ability to delay the oxidative thermal decomposition, i.e., improve the barrier properties, in nanocomposites. In this study, the maximum seems to occur for a clay loading between 1 and 5 wt %, Figure 4b, because the thermal properties are improved for the nanocomposites with 1 and 2 wt % clay and less improved with 5 wt % clay, whereas the nanocomposite with 10 wt % clay exhibits a decrease in thermal stability compared to the unfilled material. In the temperature range 100−250 °C there is a larger mass loss for the nanocomposite with 10 wt % clay compared with the other nanocomposites in both the N_2 and O_2 analyses. This mass loss probably emanates from residual water in the material, suggesting that the nanocomposite with 10 wt % clay contains a larger amount of residual water, which is in accordance with the previous discussion.

Visual inspection of the samples after TGA also gives valuable information about the thermal properties of the materials, Figure 5. After TGA under oxygen flow, the sample with the neat hyperbranched polymer has undergone almost complete combustion and there are no visible residues. For the clay-containing samples, on the other hand, the visual impression is completely different. Although the resulting weight losses obtained from the thermograms indicate that most of the materials are decomposed, the samples maintain most of their apparent size and shape; the clay nanoparticles form a skeleton-like structure that is maintained even after being subjected to oxidative combustion at 800 °C. This behavior could be very useful in fire-resistance applications (22).

3.2. Coating Characterization. Coatings were prepared both from neat Boltorn H30 resin and from the resins with 1 and 3 wt % Na^+MMT and the cross-linking showed

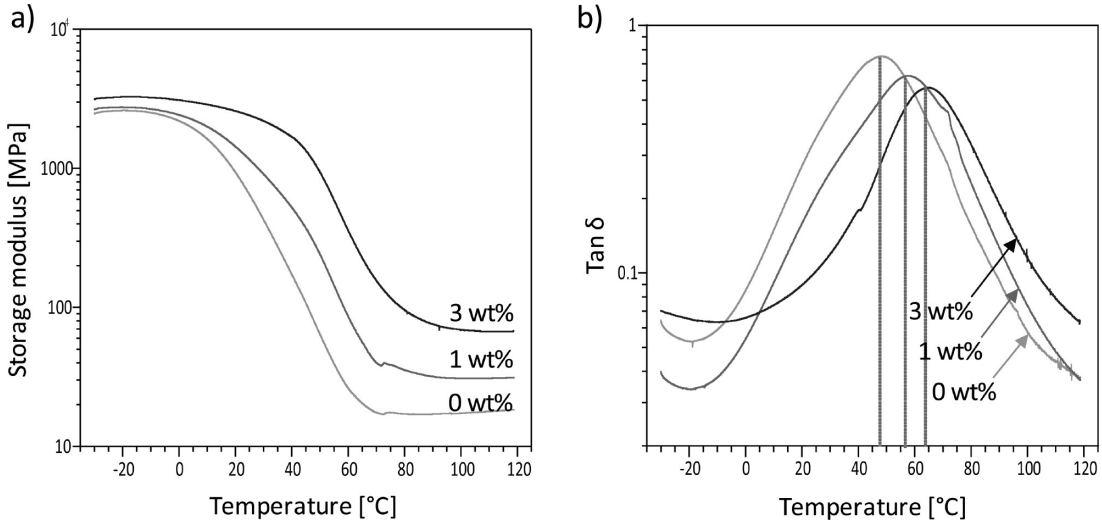

FIGURE 7. DMA results showing (a) storage modulus vs temperature, and (b) tan δ vs temperature, of Boltorn H30 coatings with 0, 1, and 3 wt % Na^+MMT.

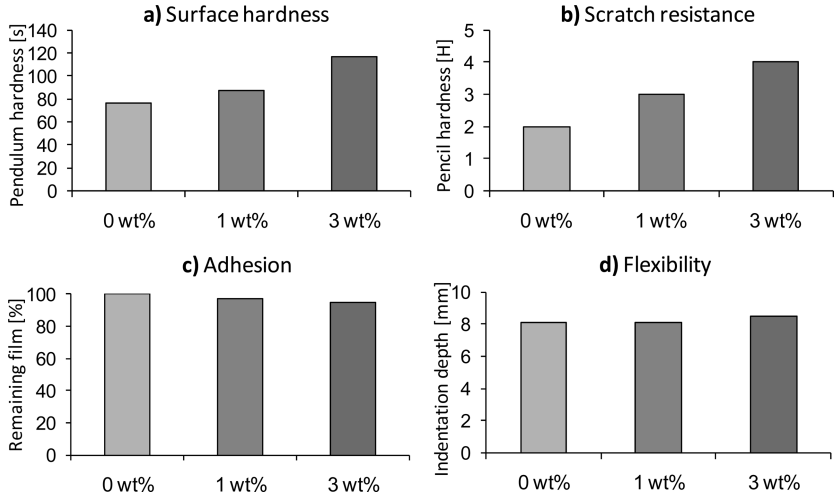

FIGURE 8. Boltorn H30 coatings with 0, 1, and 3 wt % Na^+MMT were characterized with the conventional coating characterization methods (a) pendulum hardness test, (b) pencil hardness test, (c) scratch test, and (d) Erichsen ball test, denoted by the main properties they measure.

no signs of being affected by the introduction of Na^+MMT. All coatings were smooth and appeared highly transparent under photopic vision and no discoloration could be observed. The coating in Figure 6 was prepared according to the procedure described in the Experimental section above, but with a Na^+MMT content of 2 wt %. The improved barrier properties of the nanoparticle-filled material also have a retarding effect on the drying step in the film-forming process; the clay nanosheets hinder the out-diffusion of solvent, resulting in longer required flash-off time. It is also possible that the clay nanosheets could entrap the small amounts of methanol formed during the cross-linking reaction, potentially causing bubbles and an inhomogeneous film. However, in this study no such problem occurred, possibly because of the relatively high curing temperature, which increases the mobility in the material during cross-linking.

The three different coating formulations, with and without clay, have been evaluated with respect to changes in mechanical properties induced by the introduction of the nanoparticle filler. DMA of freestanding films tested in tensile mode reveals an increase in storage modulus for the clay-containing film both above and below the T_g, Figure 7a. Furthermore there is a shift in the T_g from 48 to 57 °C and 64 °C, for 1 and 3 wt % clay, respectively, as determined by the maxima of the tan δ peaks, Figure 7b. The tan δ peak is also lowered and slightly widened with the introduction of clay, suggesting a more heterogeneous material. This implies that the clay interacts with the polymer network on a small scale, i.e., nanoscale, level; a macroscopic mixing of the filler would not give the same shift in T_g (51).

The results from the conventional coating characterization analyses are shown in Figure 8. The results from the pendulum hardness test, which measures the surface hardness in combination with the surface friction, are in concordance with the DMA results; the nanoparticle-filled coating gave rise to a higher number of pendulum swings, indicating a harder surface. According to the pencil hardness test, the addition of clay had a pronounced positive effect on the scratch resistance, and the scratch test demonstrated that

all the coatings had good adhesion to the substrate. The aim of this project was to prepare hard coatings with preserved flexibility, but the Erichsen test actually showed a slight increase in the flexibility, with the addition of clay, which was better than expected. The chemical resistance of the coatings was evaluated using the MEK-rub test, and even after more than 200 rubs all the films remained unaffected by the solvent; hence the coatings had very good chemical resistance.

4. CONCLUSIONS

Smooth and transparent coatings could be prepared from both the neat and the nanoparticle-filled hyperbranched resins. According to XRD and TEM the nanofilled coatings had a mainly exfoliated structure, and DMA also rendered indications of a nanoscale dispersion. Furthermore, the DMA showed a 9 and 16 °C increase in the T_g, for 1 and 3 wt % clay respectively, a slightly higher storage modulus—both above and below the T_g—and indications of a more cross-linked network, for the clay-containing film. TGA demonstrated the influence of the nanofiller on the thermal degradation in oxygen atmosphere. At 50% mass loss, the thermograms of the nanocomposites were shifted to approximately 40 °C higher temperature, an effect attributed to the improved barrier properties of the nanocomposites compared to the neat hyperbranched polymer. Visual inspection of the samples after TGA demonstrated the ability of the clay nanoparticles to preserve the shape of the samples even after almost complete decomposition, which could be useful in fire-resistance applications. Conventional coating characterization methods demonstrated an increase in the surface hardness, scratch resistance, and flexibility with the introduction of clay, and all coatings exhibited excellent chemical resistance and adhesion.

Acknowledgment. The Swedish Research Council (Grant 2006-3574) is gratefully acknowledged for financial support.

REFERENCES AND NOTES

(1) Ray, S. S.; Okamoto, M. *Prog. Polym. Sci.* **2003**, *28*, 1539–1641.
(2) Tjong, S. C. *Mater. Sci. Eng., R* **2006**, *R53*, 73–197.
(3) Okada, A.; Kawasumi, M.; Kurauchi, T.; Kamigaito, O. *Polym. Prepr. (ACS, Div. Polym. Chem.)* **1987**, *28*, 447–448.
(4) Usuki, A.; Kojima, Y.; Kawasumi, M.; Okada, A.; Fukushima, Y.; Kurauchi, T.; Kamigaito, O. *J. Mater. Res.* **1993**, *8*, 1179–1184.
(5) Okada, A.; Kawasumi, M.; Usuki, A.; Kojima, Y.; Kurauchi, T.; Kamigaito, O. *Mater. Res. Soc. Symp. Proc.* **1990**, *171*, 45–50.
(6) Yano, K.; Usuki, A.; Okada, A.; Kurauchi, T.; Kamigaito, O. *J. Polym. Sci., Part A: Polym. Chem.* **1993**, *31*, 2493–2498.
(7) Giannelis, E. P.; Krishnamoorti, R.; Manias, E. *Adv. Polym. Sci.* **1999**, *138*, 107–147.
(8) LeBaron, P. C.; Wang, Z.; Pinnavaia, T. J. *Appl. Clay Sci.* **1999**, *15*, 11–29.
(9) Giannelis, E. P. *Adv. Mater.* **1996**, *8*, 29–35.
(10) Vaia, R. A.; Price, G.; Ruth, P. N.; Nguyen, H. T.; Lichtenhan, J. *Appl. Clay Sci.* **1999**, *15*, 67–92.
(11) Kornmann, X.; Thomann, R.; Mulhaupt, R.; Finter, J.; Berglund, L. A. *Polym. Eng. Sci.* **2002**, *42*, 1815–1826.
(12) Lee, H.-s.; Fasulo, P. D.; Rodgers, W. R.; Paul, D. R. *Polymer* **2005**, *46*, 11673–11689.
(13) Kojima, Y.; Usuki, A.; Kawasumi, M.; Okada, A.; Kurauchi, T.; Kamigaito, O. *J. App. Polym. Sci.* **1993**, *49*, 1259–1264.
(14) Lan, T.; Pinnavaia, T. J. *Chem. Mater.* **1994**, *6*, 2216–2219.
(15) Messersmith, P. B.; Giannelis, E. P. *J. Polym. Sci., Part A: Polym. Chem.* **1995**, *33*, 1047–1057.
(16) Bharadwaj, R. K. *Macromolecules* **2001**, *34*, 9189–9192.
(17) Kim, S. H.; Kim, S. C. *J. Appl. Polym. Sci.* **2007**, *103*, 1262–1271.
(18) Blumstein, A. *J. Polym. Sci., Part A* **1965**, *3*, 2665–2672.
(19) Burnside, S. D.; Giannelis, E. P. *Chem. Mater.* **1995**, *7*, 1597–1600.
(20) Gilman, J. W.; Kashiwagi, T.; Lichtenhan, J. D. *SAMPE J.* **1997**, *33*, 40–46.
(21) Lee, J.; Giannelis, E. P. *Polym. Prepr. (ACS, Div. Polym. Chem.)* **1997**, *38*, 688–689.
(22) Gilman, J. W. *Appl. Clay Sci.* **1999**, *15*, 31–49.
(23) Alexandre, M.; Dubois, P. *Mater. Sci. Eng., R* **2000**, *R28*, 1–63.
(24) Yoon, P. J.; Fornes, T. D.; Paul, D. R. *Polymer* **2002**, *43*, 6727–6741.
(25) Wang, Z.; Pinnavaia, T. J. *Chem. Mater.* **1998**, *10*, 3769–3771.
(26) Dietsche, F.; Thomann, Y.; Thomann, R.; Mulhaupt, R. *J. Appl. Polym. Sci.* **2000**, *75*, 396–405.
(27) Strawhecker, K. E.; Manias, E. *Chem. Mater.* **2000**, *12*, 2943–2949.
(28) Kojima, Y.; Usuki, A.; Kawasumi, M.; Okada, A.; Kurauchi, T.; Kamigaito, O. *J. Polym. Sci., Part A: Polym. Chem.* **1993**, *31*, 983–986.
(29) Messersmith, P. B.; Giannelis, E. P. *Chem. Mater.* **1993**, *5*, 1064–1066.
(30) Moet, A. S.; Akelah, A. *Mater. Lett.* **1993**, *18*, 97–102.
(31) Vaia, R. A.; Vasudevan, S.; Krawiec, W.; Scanlon, L. G.; Giannelis, E. P. *Adv. Mater.* **1995**, *7*, 154–156.
(32) Kawasumi, M.; Hasegawa, N.; Kato, M.; Usuki, A.; Okada, A. *Macromolecules* **1997**, *30*, 6333–6338.
(33) Zilg, C.; Muelhaupt, R.; Finter, J. *Macromol. Chem. Phys.* **1999**, *200*, 661–670.
(34) Wu, J.; Lerner, M. M. *Chem. Mater.* **1993**, *5*, 835–838.
(35) Ogata, N.; Kawakage, S.; Ogihara, T. *J. Appl. Polym. Sci.* **1997**, *66*, 573–581.
(36) Shen, Z.; Simon, G. P.; Cheng, Y.-B. *Polymer* **2002**, *43*, 4251–4260.
(37) Chen, B.; Evans, J. R. G. *J. Phys. Chem. B* **2004**, *108*, 14986–14990.
(38) Plummer, C. J. G.; Garamszegi, L.; Leterrier, Y.; Rodlert, M.; Maanson, J.-A. E. *Chem. Mater.* **2002**, *14*, 486–488.
(39) Rodlert, M.; Plummer, C. J. G.; Garamszegi, L.; Leterrier, Y.; Grunbauer, H. J. M.; Manson, J.-A. E. *Polymer* **2004**, *45*, 949–960.
(40) Fogelström, L.; Antoni, P.; Malmström, E.; Hult, A. *Prog. Org. Coat.* **2006**, *55*, 284–290.
(41) Rodlert, M.; Plummer, C. J. G.; Leterrier, Y.; Månson, J.-A. E.; Grunbauer, H. J. M. *J. Rheol.* **2004**, *48*, 1049–1065.
(42) Hult, A.; Johansson, M.; Malmström, E. *Macromol. Symp.* **1995**, *98*, 1159–1161.
(43) Wang, Q.; Mynar, J. L.; Yoshida, M.; Lee, E.; Lee, M.; Okuro, K.; Kinbara, K.; Aida, T. *Nature* **2010**, *463*, 339–343.
(44) Malmström, E.; Johansson, M.; Hult, A. *Macromolecules* **1995**, *28*, 1698–1703.
(45) Johansson, M.; Glauser, T.; Jansson, A.; Hult, A.; Malmström, E.; Claesson, H. *Prog. Org. Coat.* **2003**, *48*, 194–200.
(46) Zagar, E.; Huskic, M.; Grdadolnik, J.; Zigon, M.; Zupancic-Valant, A. *Macromolecules* **2005**, *38*, 3933–3942.
(47) Zagar, E.; Huskic, M.; Zigon, M. *Macromol. Chem. Phys.* **2007**, *208*, 1379–1387.
(48) http://www.eastman.com/Literature_Center/M/M329.pdf (accessed April 29, 2010).
(49) Hare, C. H., *Protective Coatings.*; SSPC, The Society for Protective Coatings: Pittsburgh, PA, 1994.
(50) Hedenqvist, M. S.; Yousefi, H.; Malmström, E.; Johansson, M.; Hult, A.; Gedde, U. W.; Trollsås, M.; Hedrick, J. L. *Polymer* **1999**, *41*, 1827–1840.
(51) Paul, D. R.; Robeson, L. M. *Polymer* **2008**, *49*, 3187–3204.

AM1001986